Effects of fluid viscosity on band segregation dynamics in bidisperse granular slurries

Stanley J. Fiedor,[1] Paul Umbanhowar,[2] and Julio M. Ottino[1]
[1]*Department of Chemical and Biological Engineering, Northwestern University, Evanston, Illinois 60208, USA*
[2]*Department of Mechanical Engineering, Northwestern University, Evanston, Illinois 60208, USA*
(Received 20 February 2007; revised manuscript received 29 August 2007; published 19 October 2007)

Parallel experiments in long, axially rotated cylinders are used to study the influence of interstitial fluid viscosity on particle segregation in bidisperse granular slurries. A uniformly mixed initial state segregates into surface bands, which alternate between regions of large particles and regions composed of a mixture of small and large particles. As the tumbler rotates, the relative area of the mixed particle bands increases and saturates, while the number of bands reaches a peak and then decreases logarithmically in time for all viscosities studied. With increasing interstitial fluid viscosity, the asymptotic mixed band area increases proportionally, the time for bands to appear at the surface decreases, and the peak number of bands goes through a maximum at a viscosity of ~3 cP. Extrapolation to the low-viscosity limit matches the data for dry granular systems; at the high-end viscosity there is a value beyond which no axial banding occurs. A heuristic mechanism based on the coexistence of pure and mixed particle phases and their dependence on viscosity is presented to rationalize key aspects of the results.

DOI: 10.1103/PhysRevE.76.041303 PACS number(s): 45.70.Mg, 05.65.+b, 45.70.Qj

I. INTRODUCTION

Flowing granular materials are ubiquitous in both nature and technological applications. However, ubiquity has not yet led to a comprehensive theory, and many phenomena remain poorly understood. For example, flowing granular mixtures tend to segregate when particle properties differ [1,2]. In partially filled rotating tumblers, particles of different size or density segregate radially (perpendicular to the axis of rotation); the segregation is due to percolation for size difference and "buoyancy" for density difference [3]. For bidisperse mixtures, radial segregation typically occurs within a few rotations of the tumbler and produces a mixed small-particle-enriched core surrounded by a nearly pure large-particle region. In long tumblers and with $O(10^2)$ rotations, the mixed core can reach the surface in various locations resulting in a configuration comprised of what appear—at the free surface and boundaries of the container—to be alternating bands. This phenomenon is referred to as axial segregation.

Since the work of Oyama [4], several aspects of axial segregation have been investigated. Most studies focused on dry granular systems (DGSs), where the interstitial fluid is a gas and particles transfer momentum primarily through collisions. Gupta *et al.* [5] found that axial segregation in dry binary mixtures of different size grains occurs only if the difference in repose angles of the pure components is sufficiently large, and that the angle of repose difference is an increasing function of rotation speed. Hill and Kakalios [6] also observed a critical rotation speed above which axial segregation occurs for certain mixtures of glass particles. They reported that axial segregation is reversible and occurs when a sufficient difference exists between the repose angles of the large particles and of a mixture of large and small particles. Choo *et al.* [7] showed that transient waves of segregation can develop during the initial stages of band formation, while Nakagawa [8] and Hill *et al.* [9] observed merging of bands with increasing rotation. Fiedor and Ottino [10] observed that with increasing rotation rate there is a transition from a regime where only band merging occurs to a regime in which bands move as waves in both axial directions.

In liquid granular systems (LGSs) particles are completely immersed in a liquid, and viscous effects can potentially compete with contact-mediated interactions. Jain *et al.* [11] studied how interstitial fluid affects the flowing layer (the lenticular region of non-solid-body flow near the free surface) in tumbled monodisperse slurries. They measured flowing layer velocity profiles with interstitial fluids of air, water, and glycerin-water mixtures and found that viscosity had very little effect on particle velocity, shear rate, and flowing layer thickness. The relative importance of particle inertia as compared to viscous fluid forces is characterized by the Stokes number $\mathrm{St}=m\dot{\gamma}/6\pi\eta a$, where m is the particle mass, $\dot{\gamma}$ is the shear rate, η is the interstitial fluid viscosity, and a is the particle radius. At small St, viscous forces dominate, while at large St, particle inertia dominates. In the Jain *et al.* [11] study, St ranged from $O(10)$ for the glycerin-water mixtures to $O(10^3)$ for air. Though St varied over three orders of magnitude, particle interactions were still dominated by contact forces.

The relatively few segregation studies conducted in LGSs exhibit significant differences when compared to DGSs. Samadani and Kudrolli [12] found that segregation decreases with increasing η when completely immersed bidisperse particle mixtures are poured into a silo. They proposed that segregation is due to surface roughness and velocity fluctuations; segregation decreases with higher η because a boundary layer masks details of the surface roughness and velocity fluctuations are damped. The greater influence of viscosity (smaller St) is expected, since the particles used in these experiments have smaller m and a than those used in the Ref. [11] study. Axial segregation also shows differences between DGSs and LGSs. Jain *et al.* [13] found that axial bands in rotating tumblers form more quickly when the interstitial fluid is a liquid rather than air. Fiedor and Ottino [10] found that in LGSs the percentage of large particles in mixed bands

 ©2007 The American Physical Society

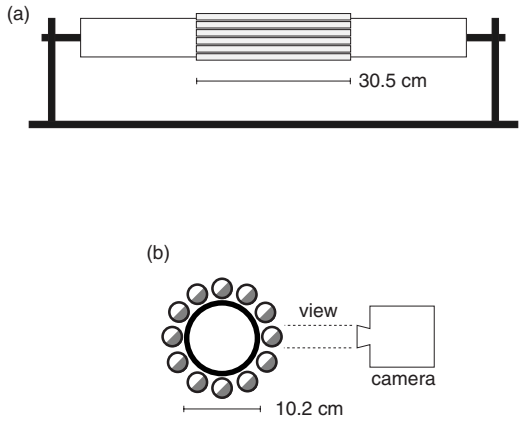

FIG. 1. Schematic of the experimental apparatus. (a) Side view of the apparatus used to investigate interstitial fluid viscosity. (b) Cross section of the apparatus. Twelve small tubes are attached to the outer wall of a larger tube.

increases as rotation rate is increased, while in DGSs, in contrast, this percentage is independent of rotation rate. The particles used in these experiments also have smaller m and a than those used in Ref. [11], which again suggests that viscosity was influential.

Another example of axial banding of granular material has previously been studied in rimming flows [14–16]. Granular particles in partially filled long cylindrical tubes can migrate and form regions of low particle concentration (or even particle-free regions) and high particle concentration. The work presented here has obvious parallels with and differences from this recent work. The differences between the rimming flow studies and this work are several and point to different physics—free surface vs completely filled tube; monodisperse particles vs mixtures of large and small particles; neutrally buoyant particles vs particles much denser than surrounding fluid. The physical models for the initial banding in the rimming flow work systems are better developed than those of axial banding of dry powders [17].

II. EXPERIMENTAL METHODS

Our axial segregation experiments are run in parallel due to the many advantages over experiments run in series [18]. Multiple tumblers are attached to the outside of a larger horizontal tube which is rotated about its axis with angular velocity ω (see Fig. 1). The tumblers rotate at the same frequency as the center tube but with some additional translation, which is negligible. The major advantage of this method is that many tumbling experiments can be run simultaneously, which significantly reduces the total experimental time.

The experimental setup consists of twelve 30.5 cm long (28 cm inner length after each end was stoppered), 1.59 cm inner diameter glass tubes filled halfway with a 1:1 volume ratio mixture of small and large glass beads. The diameter of the smaller black beads is 272 ± 24 μm, while the larger transparent bead diameter is 882 ± 30 μm. Various liquids, each with a different viscosity, fill the remaining volume of each tube. A base solution with $\eta=5.5$ cP is prepared by mixing ethanol with glycerin until the density of the mixed solution matched that of water ($\rho=1$ g/cm^3). The ethanol-glycerin mixture is then mixed with water to make liquids of various viscosities with similar density to water. In addition, pure water, ethyl alcohol, and aqueous glycerin are also used as interstitial fluids. The measured densities and viscosities of the interstitial fluids are shown in Table I. (Some additional preliminary experiments were also conducted at higher interstitial fluid viscosity to get a sense for the maximum viscosity where banding still occurs for this system.)

TABLE I. Interstitial fluid properties. EG indicates an ethanol-glycerin mixture.

	ρ (g/cm)	η (cP)	ν (10^{-2} cm^2/s)
100% EG	1.02	5.54	5.53
75% EG and 25% H_2O	1.01	3.93	3.92
50% EG and 50% H_2O	1.01	2.58	2.57
25% EG and 75% H_2O	1.00	1.68	1.68
H_2O	0.978	1.09	1.12
Ethanol	0.872	3.23	3.72
Glycerin-H_2O	1.163	6.34	5.45

The 12 glass tumblers are attached to the outside of a 76 cm long, 10.2 cm outer diameter acrylic tube that is rotated about its axis by a stepper motor at 10 rpm for $\theta=2300$ rotations. At this rate surface grain flow is continuous (individual avalanches are not evident) and the top of the flowing layer is flat. A minimum of 30 data sets were recorded for each interstitial fluid viscosity. Images of the glass tubes are acquired with a Kodak Megapixel 1.4i digital camera positioned approximately 1.5 m from the tumbler. Since suspended particulate matter and small air bubbles can obscure the view of bands on the free surface, we instead image the region of contact between the grains and the tube [see Fig. 1(b)]. The camera is synchronized to the stepper motor and images of each tube are taken once per rotation at the same angular position.

The time evolution of the axial segregation process is studied by means of space-time sequences. Images of the entire tumbler are cropped to include only the particles in the tumbler. Since there is no significant vertical variation in images of the segregation bands, each image is vertically averaged to produce a one-dimensional (1D) array of the average intensity along the tumbler. 1D arrays are concatenated into a spatiotemporal series showing all 2300 rotations of the tumbler; see examples in Fig. 2. Darker areas represent mixed regions rich in small particles, while lighter areas are essentially regions of all large particles. The narrow, horizontal, dark regions at the top of the spatiotemporal images in Fig. 2 show the initial mixed particle state.

To extract quantitative information from the images, the spatiotemporal arrays are smoothed using a two-dimensional Savitzky-Golay filter to reduce inhomogeneities due to nonuniform lighting. Next each line associated with a fixed time is independently thresholded using the average pixel value of

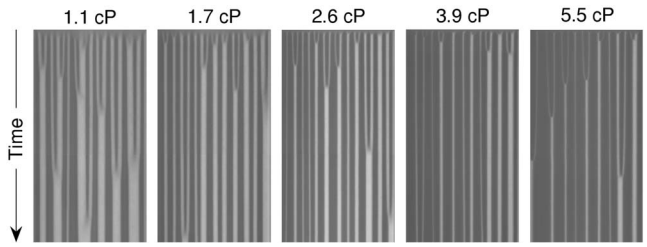

FIG. 2. Spatiotemporal images of axial segregation for interstitial fluid viscosities ranging from 1.1 to 5.5 cP. Bright areas are composed of large (clear) particles and dark regions are mixtures of large and small (black) particles. After an initial burst of band formation, the number of bands decreases monotonically as large particle bands merge. The area occupied by mixed bands increases with increasing viscosity.

the line as a reference. The result is a binary spatiotemporal image from which the number of bands and the band area are obtained.

III. RESULTS

Figure 2 shows representative examples of typical spatiotemporal images for experiments run with interstitial fluids viscosities ranging from 1.1 to 5.5 cP. The densities of the different interstitial fluids are approximately the same (~ 1 g/cm^3; see Table I). All five images show the same qualitative behavior: (1) a thin layer of large beads appears on the surface within $O(1)$ rotation, (2) mixed bands of small and large particles (dark) and mainly pure bands of large particle (bright) form, and (3) a few bands of large particles merge to form wider bands which results in fewer total bands. Unlike the case of binary DGSs [10], there is no evidence of waves or new bands after the initial interval of band formation.

Although the qualitative features of spatiotemporal band evolution are similar, there are substantial quantitative differences. Figure 3(a) shows the time evolution of the area of the mixed phase surface bands A for various interstitial fluid viscosities. Each plot is the average of 30 trials for each fluid (individual experiments show the same behavior). For all viscosities, A undergoes a period of rapid increase during the interval between 10 and 100 rotations. After this increase, A is nearly constant (with the exceptions of the fluids with $\eta = 5.54$ and 6.34) even though band merging is occurring—similar behavior was observed previously with interstitial fluids of air and water [10]. Viscosity influences a number of features of A. Of possible significance is the observation that the nearly constant value of A after the jump appears to be linear in the viscosity, as Fig. 3(b) indicates. A linear fit to the data in Fig. 3(b) gives the relative area of mixed bands after 2300 rotations as $A_{2300}(\eta) = 0.49 + 0.047\ \text{cP}^{-1}\,\eta$. Significantly, for $\eta = 0$, we obtain $A_{2300} = 0.49$ which is close to the value of ≈ 0.5 observed in DGSs in square tumblers [10]. (There has always been the question of what would happen if the axial segregation experiments took place in a vacuum.) The linear fit also predicts that there will be no bands left (i.e., $A_{2300} = 1$) when $\eta \approx 10.8$ cP. Additional experiments

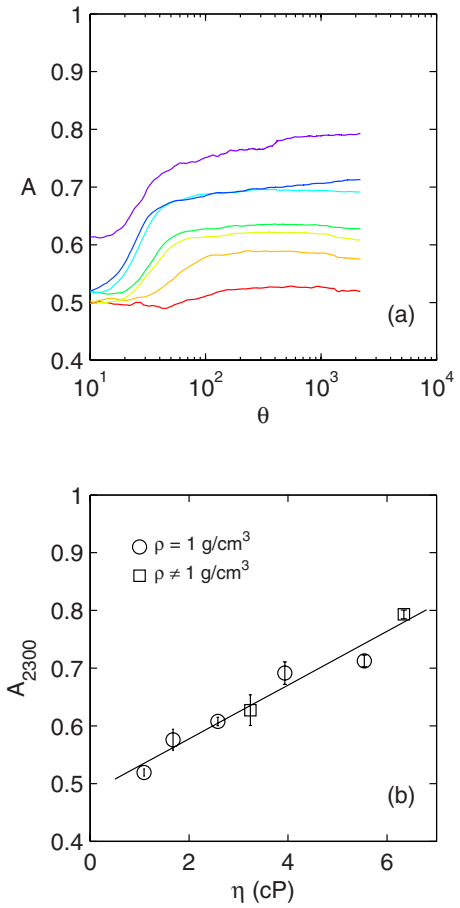

FIG. 3. (Color online) Effect of interstitial fluid viscosity on the area of mixed particle surface bands. (a) Evolution of mixed band area vs tumbler rotations for $\eta = 1.09$, 1.68, 2.58, 3.23, 3.93, 5.54, and 6.34 cP (note logarithmic axis). Mixed band area decreases monotonically with increasing η. (b) Mixed band area after 2300 revolutions plotted against interstitial fluid viscosity. The circles (○) are for interstitial fluids of the same density and the squares (□) are for ethanol and aqueous glycerin. The straight line is a best fit with $A_{2300} = 0.49 + 0.047\,\eta$.

with water-glycerin mixtures confirm that, for our experimental conditions, no band formation occurs for $\eta > 10$ cP. Another general observation is that the systems had to be well mixed initially. If any portions of the tumblers had higher local concentrations of large particles, axial bands formed in that region, implying that local concentrations control whether bands form locally. This is similar to results seen by Arndt *et al.* [19], where local fill fractions controlled band formation and dynamics. Finally, as η increases, the duration and onset time of the rapid increase in A decrease.

The segregation behavior with the highest-viscosity fluid ($\eta = 6.34$ cP) in Fig. 3(a) shows somewhat different behavior from the others. After ten rotations $A \approx 0.6$ which is much larger than for any of the other viscosities. This difference may be due to a large dark core and relatively thin large (clear) particle layer decreasing the reflected light intensity at the surface. Note that our method for locating bands (essentially thresholding) does not work when bands are not

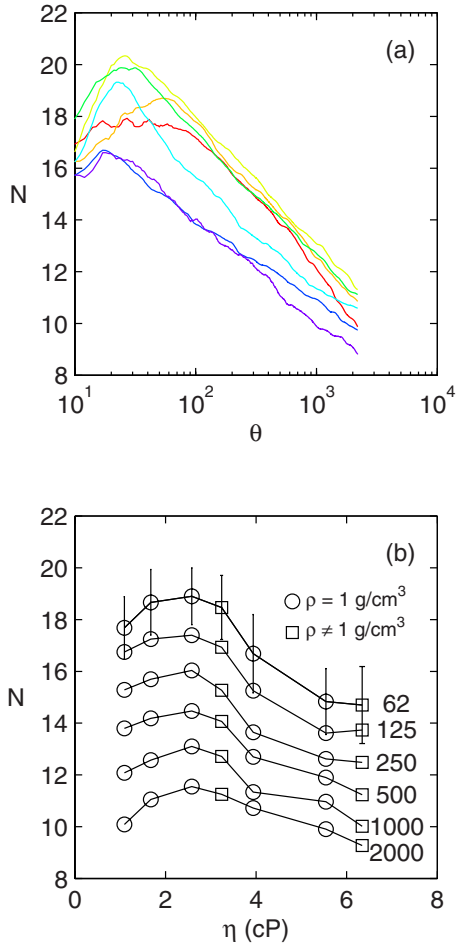

FIG. 4. (Color online) Effect of interstitial fluid viscosity on the number of mixed phase surface bands. (a) Evolution of the number of mixed phase surface bands with the number of tumbler revolutions for η=1.09, 1.68, 2.58, 3.93, and 5.54 cP. (b) Number of mixed phase surface bands vs interstitial fluid viscosity at various times during the experiments. Circles (○) are for interstitial fluids of the same density and squares (□) are for ethanol and aqueous glycerin. Error bars are included for θ=62 and are similar for other θ.

present. Therefore, we only present results after bands form (ten revolutions).

Figure 4(a) presents the evolution of the average number of mixed particle bands N versus the number of tumbler rotations, θ, for the interstitial fluids in Fig. 2. N is computed from an average of 30 experiments for each viscosity. An increase in the number of surface bands to a maximum followed by a subsequent logarithmic decrease via band merging is evident. Qualitatively similar results were previously found in experiment [10] and by numerical simulations of amplitude equations [20]. Similar to the mixed band area A, the number of tumbler revolutions at which the maximum number of bands appears decreases with increasing viscosity. The slope of N on the semilogarithmic plot appears to be largely independent of the viscosity with the exception of the data for the lowest-viscosity liquid (H_2O). Figure 4(b) shows the number of mixed phase bands versus viscosity at various times during the experiments. Unlike the monotonic response of the band area, a clear maximum in N occurs for η near 3 cP.

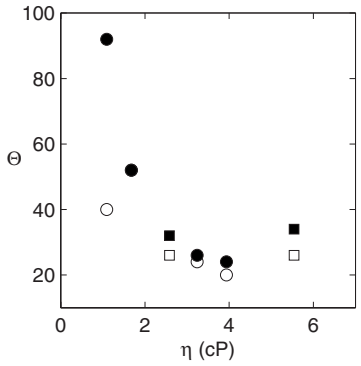

FIG. 5. Rotations Θ at which N reaches its maximum value (filled symbols) and at which A first exceeds $(A_{max}+A_{min})/2$ (open symbols) vs fluid viscosity. Symbols ○ and □ indicate fluid density as in Fig. 4(b).

As mentioned previously, the required number of tumbler rotations for the area to reach a steady state and for the number of bands to peak decreases with increasing viscosity. Figure 5 plots the number of rotations Θ_A and Θ_N, respectively, at which these two events occur as a function of viscosity. Filled symbols indicate when N reaches its maximum value while open symbols show when A first exceeds $(A_{max}+A_{min})/2$. At η=0 we expect our results to match the finite values associated with DGSs while for $\eta\rightarrow\infty$ we expect θ to become a constant.

IV. DISCUSSION

The results presented generate a large number of questions. A full theoretical explanation lies in the future. A comparison with two somewhat related cases is valuable: segregation in rimming flows and axial segregation of dry granular matter. Models for rimming flows [17] are essentially predictive, whereas those of dry matter are less developed. There is no theoretical guidance in the case of the results presented in this paper. We offer a heuristic argument that, while incomplete, fits several of the observations reported in this work. First let us review a few of the most relevant results.

After $O(100)$ rotations, the surface of the bed is divided into distinct bands of large particles and mixed (small and large) particles as sketched in Fig. 6. The relative particle concentrations within the mixed bands is constant in time and independent of axial position, while the large particle bands are nearly pure. Consider, however, that a vertical slice through the middle of a mixed band at a fixed axial position apparently resembles the initial condition—a uniformly mixed collection of large and small particles. Why do large particles not segregate further from the small as they do initially? The primary difference with the initial condition is that the concentration of the large particles has been reduced. Evidently, if the relative concentration of large to small particles is sufficiently reduced, there is no segregation. Accordingly, we speculate that there is a maximum concentration of

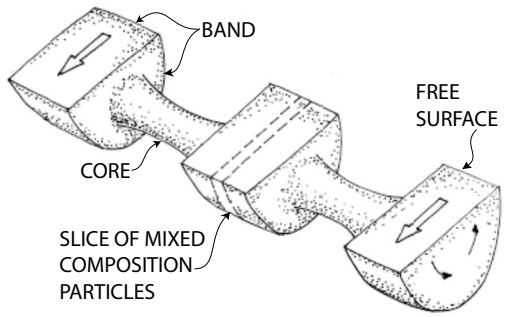

FIG. 6. Schematic illustrating the location and motion (arrows) of mixed material in the tumbler after bands appear. Mixed particles form a continuous volume composed of surface bands connected by a subsurface core. Nearly homogeneous bands of large particles (not shown) occupy the topologically toroidal regions outside the core between the mixed bands.

large particles that can be "dissolved" in the small particles. For a solid dissolved in a liquid, such as salt in water, the maximum solute concentration depends on temperature and the nature of the solute, while for tumbled granular materials, the maximum solute concentration would appear to depend on interstitial fluid viscosity, rotation rate, and the relative size and density of the particles. Continuing with this analogy, the initial conditions in our experiments correspond with unstable supersaturated solutions in which the large particles quickly precipitate out of the mixed phase.

In our experiments, the particles are initially well mixed with a 1:1 ratio by volume of larger and smaller particles. Imagine the mixture as being a mixed phase with an initial concentration of large particles $C_{L,0}$, where C_L is the concentration of the larger particles. Within 1–2 rotations, radial segregation occurs resulting in a two-phase system—a mixed phase at the core with $C_L < C_{L,0}$ and a pure phase at the periphery extending uninterrupted along the length of the tumbler. The pure phase consists of large particles while the mixed phase consists of large and small particles with $C_L < C_{L,0}$. Subsequently, a total volume is associated with each phase, V_P for the pure phase and V_M for the mixed phase. We suggest that, after the initial radial segregation occurs, no further segregation takes place; i.e., V_P, V_M, and C_L remain constant. Axial bands form due to an as of yet unidentified instability in which the mixed core penetrates the large particles and subsequently appears at the surface. However, as the mixed particle core grows radially at some axial locations it must shrink in others if V_M is to be preserved. Below, we examine our experimental results in light of this perspective.

Our results and previous work [10] indicate that A remains nearly constant after band formation [Fig. 3(a)]. When large (pure) particle bands merge, the intraband mixed phase must move down toward the core and up from the core on the edges of the newly joined pure band if both A and V_M are to remain constant. So during the merger the same volume of the mixed phase should move to and from the core simultaneously. Our results also indicate that A increases with η. A similar relationship is seen with the mixed phase in LGSs at different rotation rates [10]. Since the pure phase bands consist of only large particles regardless of the interstitial fluid, two scenarios could result in A increasing with η. Either C_L increases in the mixed phase, or more of the mixed phase moves out from the core to the surface (deeper pure phase bands).

The time for bands to appear at the surface is dependent on η (Fig. 5). Within a few rotations the mixed phase forms a core throughout the tumbler. C_L increases with higher η, resulting in a larger core. Bands appear at the surface when the core grows sufficiently to pierce the surface. In a system with a larger core, less growth is necessary for bands to appear at the surface. Thus, in systems with higher η, bands appear faster because less core growth is needed to reach the surface.

The viscosity of the interstitial fluid has a nonmonotonic effect on the number of bands that form initially, N_0. Since we have posited that C_L increases with η, a larger value of η produces a thinner pure layer surrounding the mixed core (smaller V_L). If we assume that the characteristic length scale of the bands at the onset of segregation is related to the initial pure layer thickness, our findings of increasing N_0 with η are consistent with our model. However, for viscosities above ~ 3 cP, N_0 decreases. Consider that the velocities of particles in the mixed phase bands are higher than those in the pure phase bands, because smaller particles flow faster in rotating tumblers [11,21]. Thus a higher local shear exists in the particle and fluid flow at the band interfaces. Increasing the interstitial fluid viscosity decreases the velocity difference of particles in the two bands due to increased C_L in the mixed phase and higher resistance in the fluid. We speculate that this decrease in the velocity difference may repress band formation, resulting in fewer initial bands in fluids with η higher than approximately 3 cP. It is clear that further experimentation is necessary to provide support for this heuristic argument.

V. CONCLUSIONS

We have studied the influence of interstitial fluid viscosity on band formation and dynamics in bidisperse granular slurries in long, axially rotated cylinders. An initially uniform mixed state develops into alternating surface bands of large particles and a mixture of large and small particles. The relative area of the mixed bands saturates with tumbler rotation. The mixed band area increases linearly with viscosity while the time for bands to appear at the surface decreases with increasing viscosity. In contrast, the number of bands reaches a maximum value and then decreases logarithmically in time. The number of bands is maximum for an interstitial fluid viscosity of approximately 3 cP.

A proposed mechanism based on phase coexistence between pure and mixed grain states explains many aspects of our results. Radial segregation occurs within 1–2 rotations, creating a two-phase system. The core is comprised of the mixed phase, a mixture of small and large particles, and the periphery is comprised of the pure phase (large particles only). The concentration of large particles in the mixed phase depends on the interstitial fluid viscosity; at higher viscosity the mixed phase is more contaminated with large particles, resulting in a larger volume of the mixed phase and a larger

core. Bands form when the core grows sufficiently to penetrate the pure phase surface and larger cores need less growth to reach the surface. Thus bands appear faster with higher viscosities. Also, a larger volume of the mixed phase allows more bands to form, but at higher viscosities viscous coupling reduces the number of bands.

Our experimental findings and the solubility analogy point the way to further experimental and theoretical developments addressing granular segregation. Pure radial segregation experiments (to avoid the added complications of axial band formation) with varying particle size ratios, densities, and relative concentrations, tumbler rotation rates, and fluid viscosities and densities would be one way to test our solubility hypothesis. However, end effects must be taken into account or minimized. If successful, fruitful connections to thermodynamic analogs seem possible. Further experiments tracking individual particle motion using index matching, magnetic resonance imaging, x-ray, or positron emission tomography techniques would shed light on the proposed instability leading to axial band formation.

[1] H. A. Makse, S. Havlin, R. K. King, and H. E. Stanley, Nature (London) **386**, 379 (1997).
[2] K. M. Hill, D. V. Khakhar, J. F. Gilchrist, J. J. McCarthy, and J. M. Ottino, Proc. Natl. Acad. Sci. U.S.A. **96**, 11701 (1999).
[3] N. Jain, J. M. Ottino, and R. M. Lueptow, Phys. Rev. E **71**, 051301 (2005).
[4] Y. Oyama, Sci. Pap. Inst. Phys. Chem. Res. (Jpn.) **37**, 17 (1940).
[5] S. Das Gupta, D. V. Khakhar, and S. K. Bhatia, Chem. Eng. Sci. **46**, 1513 (1991).
[6] K. M. Hill and J. Kakalios, Phys. Rev. E **52**, 4393 (1995).
[7] K. Choo, T. C. A. Molteno, and S. W. Morris, Phys. Rev. Lett. **79**, 2975 (1997).
[8] M. Nakagawa, Chem. Eng. Sci. **49**, 2540 (1994).
[9] K. M. Hill, A. Caprihan, and J. Kakalios, Phys. Rev. E **56**, 4386 (1997).
[10] S. J. Fiedor and J. M. Ottino, Phys. Rev. Lett. **91**, 244301 (2003).
[11] N. Jain, J. M. Ottino, and R. M. Lueptow, J. Fluid Mech. **508**, 23 (2004).
[12] A. Samadani and A. Kudrolli, Phys. Rev. E **64**, 051301 (2001).
[13] N. Jain, D. V. Khakhar, R. M. Lueptow, and J. M. Ottino, Phys. Rev. Lett. **86**, 3771 (2001).
[14] O. A. M. Boote and P. J. Thomas, Phys. Fluids **11**, 2020 (1999).
[15] M. Tirumkudulu, A. Mileo, and A. Acrivos, Phys. Fluids **12**, 1615 (2000).
[16] G. Plantard, H. Saadaoui, P. Snabre, and B. Pouligny, Europhys. Lett. **75**, 335 (2006).
[17] B. Jin and A. Acrivos, Phys. Fluids **16**, 641 (2004).
[18] S. J. Fiedor, P. Umbanhowar, and J. M. Ottino, Phys. Rev. E **73**, 041303 (2006).
[19] T. Arndt, T. Siegmann-Hegerfeld, S. J. Fiedor, J. M. Ottino, and R. M. Lueptow, Phys. Rev. E **71**, 011306 (2005).
[20] I. S. Aranson, L. S. Tsimring, and V. M. Vinokur, Phys. Rev. E **60**, 1975 (1999).
[21] N. Jain, J. M. Ottino, and R. M. Lueptow, Phys. Fluids **9**, 31 (2002).